# Proton Spectra from the Nitrogen Bombardment of Fluorine

C. E. HUNTING*

*Oak Ridge National Laboratory,† Oak Ridge, Tennessee*

(Received March 13, 1961)

Energy spectra and absolute differential cross sections of protons from bombardment of $F^{19}$ with 21.4- and 27.4-Mev $N^{14}$ were measured. The energy spectra were analyzed in terms of the statistical model with a level density $\exp(E^*/T)$, where $E^*$ is the excitation energy in the residual nucleus of the assumed reaction $F^{19}(N^{14},p)P^{32}$. The nuclear temperature $T$ increased from about 1.9 Mev at 0° to about 2.5 Mev at 145° c.m., but did not vary with bombarding energy. The angular distributions show minima near 90° c.m., with anisotropy increasing as the bombarding energy and proton energy increase. At the lower bombarding energy there is approximate agreement with the Ericson-Strutinski theory of angular-momentum effects in compound-nucleus processes, over the entire observed ranges of angle and proton energy. The fit is consistent with $\sigma=3$ in the nuclear level spin distribution $(2j+1)\exp[-j(j+1)/(2\sigma^2)]$. At the higher bombarding energy a considerable excess of protons are emitted into the backward hemisphere, especially at high proton energies, suggesting a direct-interaction mechanism in which the observed proton comes from the $F^{19}$.

## I. INTRODUCTION

REACTIONS induced by heavy ions in which most of the nuclear matter fuses together and in which de-excitation takes place exclusively by the emission of light particles $(1 \leq A \leq 4)$ and $\gamma$ rays provide a unique tool in the field of low- and medium-energy nuclear reactions. The low velocity of the colliding particles and the drastic nucleon rearrangements which must take place in such reactions are particularly conducive to the compound-nucleus process, in which many degrees of freedom of the nuclear system participate.[1,2] For this reason such reactions may be used in the search for limits of application of direct-interaction processes,[3] which involve only a few degrees of freedom of the nuclear system. For example, $F^{19}$ bombardment with 27-Mev $N^{14}$ nuclei produces a compound-system excitation energy of 44 Mev with an incident velocity less than that of a 2-Mev proton, and with more than two-thirds of the excitation energy provided by the $Q$ value.

Among the ways that light-particle emission from heavy-ion-induced reactions have been studied are the following, given with current interpretations:

(1) Excitation functions have been determined for radioactive residual nuclei which can be produced only by such reactions. At bombarding energies near 2 Mev per nucleon these have been interpreted as being generally consistent with the compound-nucleus mechanism[4]; the admixture of other reaction mechanisms is indicated for bombarding the energies near 10 Mev per nucleon.[2]

(2) The shape of the energy spectrum of the emitted

light particles themselves has been investigated. At bombarding energies near 10 Mev per nucleon as well as near 2 Mev per nucleon, the results are in at least qualitative agreement with the predictions of the compound-nucleus theory.[1,5-8]

(3) Angular distributions of the emitted light particles have been measured at bombarding energies near 10 Mev per nucleon.[8,9] The compound-nucleus theory prediction of symmetry about 90° in the center-of-mass (c.m.) system was approximately satisfied for the observed protons, while for alpha particles a considerable excess of particles emitted in the forward hemisphere suggested a direct interaction mechanism. At bombarding energies near 2 Mev per nucleon, angular distributions of the emitted light particles have been measured only for laboratory angles less than 90°. At both bombarding energies, the alpha-particle angular distributions display markedly more anisotropy than the proton angular distributions.

The object of this paper is to describe angular and energy distributions of protons emitted from reactions induced in $F^{19}$ by $N^{14}$ ions with about 2 Mev per nucleon, in the laboratory angular range 0°–140°.

Motivation for this work has been increased by the extension of the above-mentioned prediction of symmetry about 90° to a quantitative prediction of the entire angular distribution, on the basis of angular momentum effects in light-particle emission from com-

* Now at the Physics Program Office, National Science Foundation, Washington 25, D. C.

† Operated for the U. S. Atomic Energy Commission by Union Carbide Nuclear Company.

[1] C. D. Goodman, Bull. Am. Phys. Soc. **2**, 52 (1957); C. D. Goodman and J. L. Need, Phys. Rev. **110**, 676 (1958)

[2] A. Zucker, Ann. Rev. Nuclear Sci. **10**, 27 (1960).

[3] For recent developments see, for example, *Proceedings of the International Conference on Nuclear Structure, Kingston, August 29–September 3, 1960*, edited by D. A. Bromley and E. W. Vogt (University of Toronto Press, Toronto, 1960), Chap. 4.

[4] R. Nakasima, Y. Tanaka, and K. Kikuchi, Progr. Theoret. Phys. (Japan) **15**, 574 (1956).

[5] A. Zucker, Nuclear Phys. **6**, 420 (1958).

[6] C. D. Goodman and A. Zucker, in *Proceedings of the Conference on Reactions Between Complex Nuclei, Gatlinburg, Tennessee, May 5–7, 1958*, [Oak Ridge National Laboratory Report, ORNL-2606 (unpublished)], pp. 94–134.

[7] M. L. Halbert and A. Zucker, Phys. Rev. **114**, 132 (1959).

[8] W. J. Knox, A. R. Quinton, and C. E. Anderson, Phys. Rev. Letters **2**, 402 (1959), and Phys. Rev. **120**, 2120 (1960); W. J. Knox, in *Proceedings of the Second Conference on Reactions Between Complex Nuclei, May 2–4, 1960, Gatlinburg, Tennessee* (John Wiley & Sons, Inc., New York, 1960), p. 263.

[9] D. M. Parfanovich, N. V. Rabin, and A. M. Semchinova, quoted by G. N. Flerov, in *Proceedings of the Second United Nations International Conference on the Peaceful Uses of Atomic Energy, Geneva, 1958* (United Nations, Geneva, 1958), Vol. 14, p. 151.
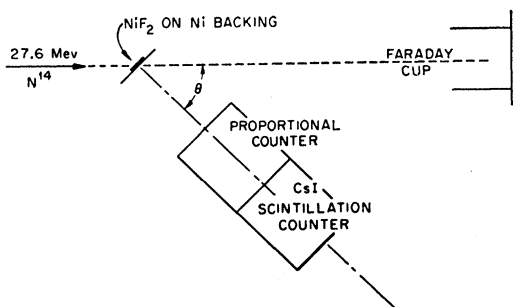
FIG. 1. Schematic diagram of experimental equipment.

pound nucleus processes.[10] This prediction has already been used, for example, to interpret angular distributions of light particles from reactions induced by 10 Mev per nucleon $O^{16}$ ions,[8] as well as to interpret angular correlations between the emitted protons of the reaction $Ni^{58}(\alpha,2p)$.[11]

## II. EXPERIMENTAL

The experimental apparatus is shown schematically in Fig. 1. The beam of 27.9-Mev nitrogen ions from the ORNL 63-in. cyclotron entered a 24-in. diam scattering chamber,[12] passed through the fluorine target, and was monitored by a Faraday cup. Particles from reactions in the target struck a proportional counter–scintillation counter telescope, which, with the associated electronics, selected the reaction protons and measured their energy.

Serving as fluorine targets were 0.2-mg/cm² layers of $NiF_2$ obtained by the exposure of fluorine gas to nickel plates at high temperatures. The remaining metallic nickel was then etched off, and the $NiF_2$ layers were transferred onto 1-mg/cm² nickel foils. Since the Coulomb barrier for $N^{14}$ ions on nickel is considerably above the bombarding energy, there was no light-particle emission due to the nickel.

Mounted entirely within the scattering chamber with the target was the counter telescope (Fig. 2). Its short length ($7\frac{1}{4}$ in.) was due primarily to the use of selected six-stage DuMont 6365 photomultiplier tubes. An auxiliary experiment using elastically-scattered 22-Mev protons showed that these photomultiplier tubes were capable of a resolution at least as good as 3.5% full-width at half-maximum. The counter telescope itself, utilizing a CsI(Tl) scintillator, had an energy resolution of about 10% full-width at half-maximum for 19-Mev protons, as shown by the energy calibration spectra. The angular resolution of the target-counter system was equivalent to that of a cone of half-angle 2°.

The proportional counter was filled to a pressure of 2 atm with the gas mixture 90% argon, 10% methane. To prevent heavily-ionizing particles from saturating



FIG. 2. Sectional view of the proportional counter-scintillation counter telescope used.

the proportional counter a 4.3-mg/cm² nickel absorber was attached in front of the counter; this was made a total of 28.5-mg/cm² aluminum equivalent between the $NiF_2$ and the crystal.

The particle-selective scheme has been described by Goodman and Need[1] and involves the simultaneous display of the proportional counter and scintillation counter outputs as $x$ and $y$ coordinates on an oscilloscope face. A block diagram of the electronics for the present experiment is shown in Fig. 3. For pulse amplification the doubly-differentiating A-8 preamplifier and amplifier system[13] was chosen because its high gain and low noise level compensated the comparatively low gain of the six-stage photomultipliers used. For the timing pulse the cross-over-pickoff gate pulse generator[14] was used to increase the time resolution of the "$Z$-axis" unblanking pulse.

Since the gain of the scintillation-counter amplifier could not be changed during the course of a day's run without a lengthy readjustment of the particle-selective system, it was found convenient to amplify the scintillation-counter signal in two parallel amplifiers, one of which had been modified to continuous gain control.

Energy calibration of the observed spectra was through the known $Q$ values of $N^{14}(d,p)N^{15}$ transitions to the ground and 6.33-Mev states in $N^{15}$. Here the $N^{14}$ beam was incident on approx. 0.1-mg/cm² solid deuterated-polyethylene targets. These were prepared by dis-

[10] T. Ericson and V. Strutinski, Nuclear Phys. 8, 284 (1958); 9, 689 (1958–59).

[11] D. Bodansky and I. Halpern, University of Washington Cyclotron Progress Report for Year Ending June 15, 1960 (unpublished), p. 24.

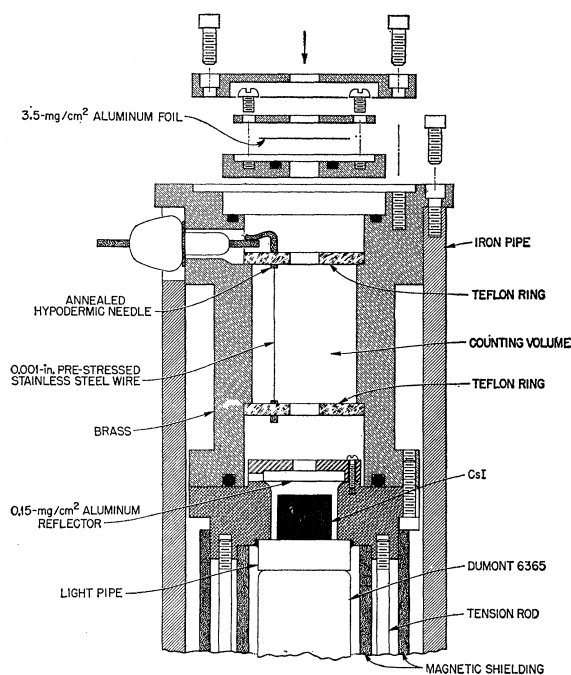[12] M. L. Halbert, C. E. Hunting, and A. Zucker, Phys. Rev. 117, 1545 (1960).

[13] G. G. Kelley, IRE Natl. Conv. Record, Part 9, 63 (1957).

[14] E. Fairstein, in ORNL Instrumentation and Controls Division Annual Progress Report for Period Ending July, 1957, Oak Ridge National Laboratory Rept. ORNL-2480 (unpublished), p. 1.
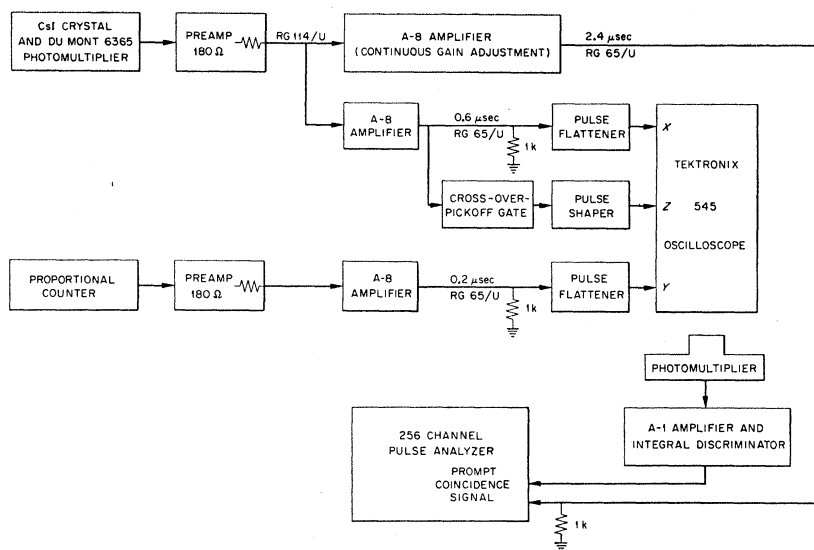
FIG. 3. Block diagram of electronic circuitry.

solving the deuterated polyethylene[15] in hot kerosene, keeping the solution hot during transfer to 1-mg/cm² Ni foil backing and during evaporation of the kerosene solvent. Due to the loss of deuterium from these targets
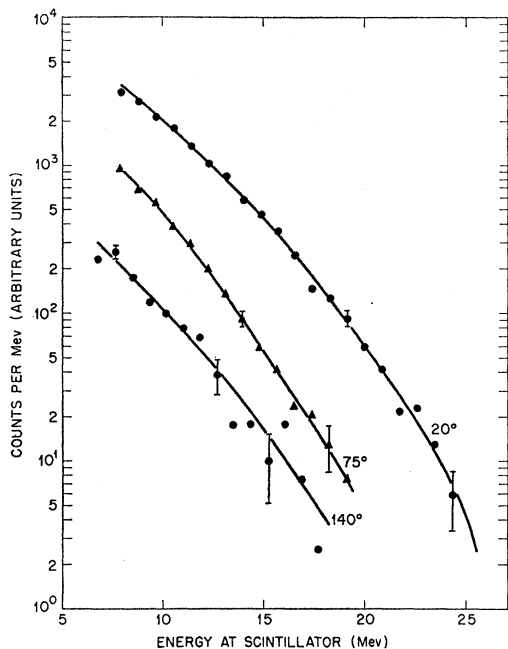


FIG. 4. Representative laboratory-system energy spectra of protons from $F^{19}$ bombardment by 27.4-Mev $N^{14}$ ions. The 28.5-mg/cm² aluminum-equivalent absorber between the center of the target and the front of the scintillation counter has not been corrected for in this figure, but the normalization of the curves to each other is experimental and not arbitrary. The large effect of the center-of-mass motion is quite evident. To improve the statistics of the individual points in this figure, each point represents eight channels on the multi-channel analyzer.

during $N^{14}$ bombardment, a new deuterium target was used for each energy calibration run.

Angular distributions were obtained in the following manner. Since the $NiF_2$ targets were nonuniform, the counting rates varied slightly, depending upon the position of the beam intersection with the target. To compensate for this effect, alternate runs were taken at 90° in the laboratory system, without moving the target. Data were accepted only where a series of 90° runs all agreed to within 10%; with the aid of the beam monitor all energy spectra were normalized to that at 90°. The target was tilted at 45° toward or away from the counter according as the counter angle was less than or greater than 90°. For the experiment at 21.4-Mev bombarding energy a 1.17 mg/cm² nickel-foil absorber was mounted on the target frame directly in front of the $NiF_2$ target, the beam entering the absorber at a 45° angle. From previous experience[12] and from the theory of small-angle scattering,[16] the degrading foil caused only a negligible decrease in the angular resolution.

In taking the data at the 27.4-Mev bombarding energy in the angular range 0°–15°, a 5.75 mg/cm² nickel foil was mounted on the target frame to stop the beam after it passed through the target, which was normal to the beam in this case. This shielded the counter telescope from the direct $N^{14}$ beam. A heavy aluminum foil formed the sides of a Faraday cup on the beam side of the target holder for monitoring the beam at the target. in this series of runs alternate spectra were taken at 20°, permitting normalization of the 0°, 5°, and 10° runs in the manner described above.

The beam energy at the center of the target was calculated from the known beam energy[17,18] and from

[15] Obtained from the Isotopes Division of Oak Ridge National Laboratory.

[16] B. Rossi, *High-Energy Physics* (Prentice-Hall, Englewood Cliffs, New Jersey, 1952), p. 66.

[17] H. L. Reynolds, D. W. Scott, and A. Zucker, Phys. Rev. **95**, 671 (1954).

[18] M. L. Halbert and J. L. Blankenship, Nuclear Instr. and Meth. **8**, 106 (1960).

the known stopping power of nickel for nitrogen ions.[17] At each bombarding energy, the $N^{14}$ energy at the center of the target was confirmed to within 0.4 Mev by means of the $N^{14}(d,p)N^{15}$ reaction described above.

Absolute differential cross sections were estimated from the known beam current and geometry and the estimated target thickness. The target thickness was estimated from x-ray measurements of the $NiF_2$ layer before the metallic nickel backing was etched off. For this estimate an x-ray beam was diffracted from the underlying metallic nickel layer, and its attenuation in the $NiF_2$ layer was compared with known attenuation coefficients.[19]

## III. RESULTS

Experimental results include proton spectra at laboratory angles of 20°, 30°, 60°, 75°, 90°, 105°, 120°, and 140° from reactions induced in the $F^{19}$ target by nitrogen ions at 27.4- and 21.4-Mev laboratory energy. In addition, proton spectra were obtained at the higher bombarding energy at laboratory angles of 0°, 5°, 10°, and 20°, and were normalized to the other results at 20°. Examples of these results are shown in Figs. 4 and 5.

The observed proton spectra were converted into the center-of-mass system of the colliding $N^{14}$ and $F^{19}$ nuclei by means of computer codes.[20] An example of a
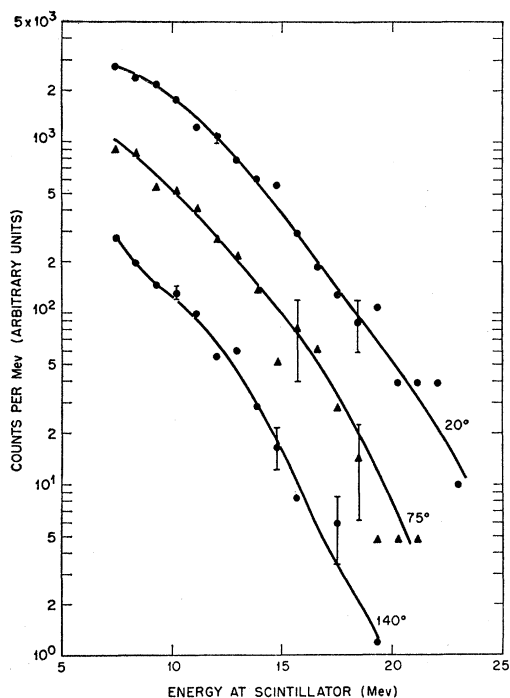
FIG. 5. Laboratory-system energy spectra of protons from reactions induced in $F^{19}$ by 21.4-Mev $N^{14}$ ions. For interpretation see the caption of Fig. 4.
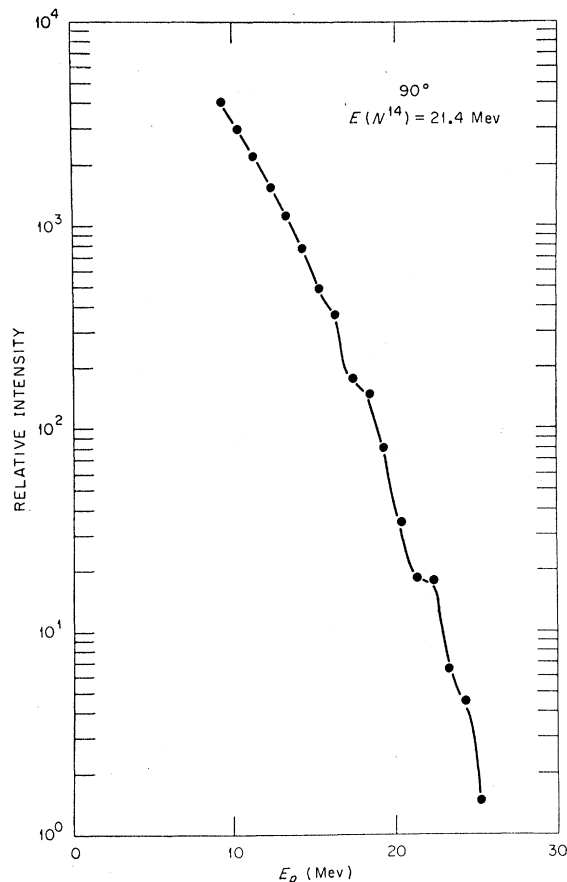
FIG. 6. An example of an energy spectrum in the c.m. system of protons from $F^{19}$ bombardment with 21.4-Mev $N^{14}$ ions. The laboratory angle in this case is 90°.

spectrum in the center-of-mass system is shown in Fig. 6 where the proton energy $E_p$ does not include recoil energy. From these spectra differential cross sections were obtained for protons of fixed kinetic energy in the center-of-mass system, as shown in Figs. 7 and 8. The errors as shown include effects of statistics, normalization between angles, and an observed nonreproducibility of about 30% at the high-energy end of the proton spectra at the higher bombarding energy. The estimated error in the absolute differential cross section for the 27.4-Mev data is ±50%. For the 21.4-Mev data, the absolute differential cross section was measured only relative to that for the 27.4-Mev data, and with an additional error of about ±30%.

## IV. ASSUMPTIONS OF THE STATISTICAL MODEL

Conditions for the simple predictions of statistical reactions[21,22] are as follows:

[19] Thanks are due to F. L. Ball, E. J. Barber, F. N. Bersey, and C. F. Hale, all of Union Carbide Nuclear Company, for preparing the target material and for measuring its thickness.
[20] C. D. Goodman and B. D. Williams, Oak Ridge National Laboratory Rept. ORNL-2925, May, 1960 (unpublished). Center-of-mass angles were determined using the code described in B. D. Williams, Oak Ridge National Laboratory Rept. ORNL-2963, December, 1960 (unpublished).
[21] W. Hauser and H. Feshbach, Phys. Rev. 87, 366 (1952).
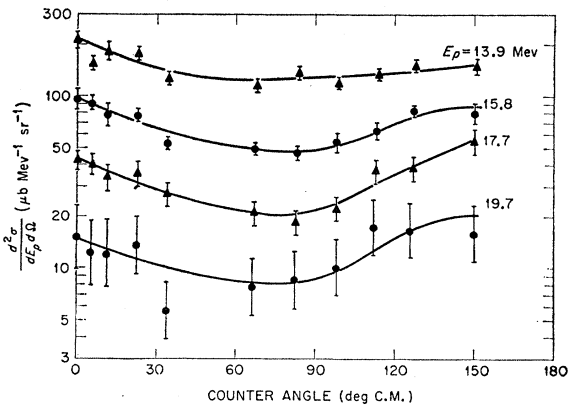[22] T. Ericson, reference 3, p. 697.

FIG. 7. Angular distributions of protons of kinetic energy $E_p$ from $F^{19}$ bombardment by 27.4-Mev $N^{14}$ ions. The c.m. system is that of the initial $N^{14}-F^{19}$ collision. Note that the recoil energy is not included in the proton kinetic energy.

(1) The reaction should proceed by a compound nucleus process.[23] This process would be suggested by a low velocity of the colliding particles and a short mean free path for absorption into a compound system. From optical model calculations[12] this mean free path is approximately 0.5 f, about one-twelfth of the 6-f interaction distance in this case.

(2) The experiment should average out fluctuations due to properties of individual compound states and due to the finite emission width. In other words, it is assumed that $\Delta E_i \gg \bar{D}$ and $\Delta E_i \gg \hbar/\tau_c$, where $\Delta E_i$ is the energy interval in the compound system averaged over by the beam energy spread and target thickness, $\bar{D}$ is the average spacing of levels which are excited in the compound nucleus, and $\tau_c$ is the mean lifetime of the compound system. Since experimentally $\Delta E_i \cong 2$ Mev, from neutron resonance work[24] it is expected that the first inequality is satisfied very well. The second inequality can be rewritten $\tau_c \gg \hbar/\Delta E_i = $ (here) $3 \times 10^{-22}$ sec. By chance $3 \times 10^{-22}$ sec is very close to the transit
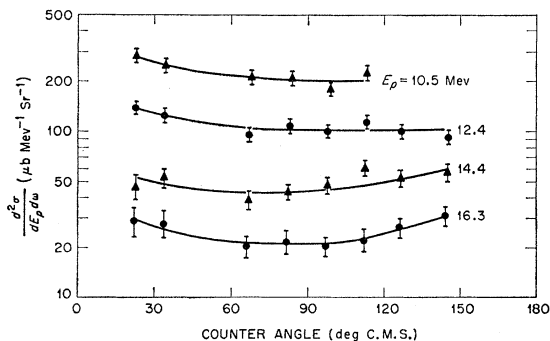
time for the initial collision, so that the second inequality reduces to condition (1).

(3) That the observed particles are all boiled off from the same residual nucleus. (This assumption is made for simplicity, and is not essential to the model itself.) The results of this experiment were interpreted in terms of the reaction $F^{19}(N^{14},p)P^{32}$, although it was not feasible to obtain good counting statistics of protons of energy greater than the maximum possible proton energy from other $F^{19}-N^{14}$ reactions. The effect of weakening this assumption can be discussed more easily (Sec. VII) following an analysis using this assumption. We note here that a statistical model calculation by Fraenkel[25] predicts that, for the upper three-fourths of the reported proton energy range at each bombarding energy, essentially all of the emitted protons correspond to the residual nucleus $P^{32}$. The prediction specified the order of emission, with the high-energy protons preceding rather than following the emission of other particles.

## V. FITS TO ENERGY SPECTRA

With the above assumptions, Hauser and Feshbach[21] predict that the proton energy spectra should reflect the level density in the residual nucleus. That is,

$$N(\epsilon)d\epsilon = \text{const}\,\epsilon\sigma_c(\epsilon)\mathcal{W}(E^*)d\epsilon, \qquad (1)$$

where $N(\epsilon)d\epsilon$ is the number of observed particles of channel energy $\epsilon$ in energy interval $d\epsilon$. The cross section for formation of a compound nucleus by the inverse process, $\sigma_c(\epsilon)$, was calculated from the asymptotic formula of Blatt and Weisskopf[26]; since $\epsilon$ is greater than twice the classical Coulomb barrier for all the data reported here, this factor had little effect. The excitation energy in the residual nucleus is $E^* = \epsilon_{max} - \epsilon$, where $\epsilon_{max}$ is listed in Table I. $\mathcal{W}(E^*)$ is the level density of the residual nucleus.

The simple theoretical level density formula given



FIG. 8. Center-of-mass system angular distributions of protons of kinetic energy $E_p$ from $F^{19}$ bombardment by 21.4-Mev $N^{14}$ ions.

TABLE I. Energies and angular momenta in the reaction $F^{19}(N^{14},p)P^{32}$. Column (1) gives the bombarding energies in the laboratory system. The corresponding excitation energies in the compound nucleus follow in column (2), while column (3) lists the mean-square orbital angular momentum of the $F^{19}-N^{14}$ collision, calculated as in the Appendix. Column (4) gives the maximum proton channel energy energetically possible at each bombarding energy.

| (1) $E(N^{14})$ (Mev) | (2) $E_{cn}^*$ (Mev) | (3) $\langle I(I+1)\rangle$av | (4) $\epsilon_{max}$ (Mev) |
|---|---|---|---|
| 21.4 | 40.4 | 33.7 | 30.8 |
| 27.4 | 43.9 | 74.1 | 34.2 |

[23] J. M. Blatt and V. F. Weisskopf, *Theoretical Nuclear Physics* (John Wiley & Sons, New York, 1952), p. 341.

[24] P. M. Endt and C. M. Braams, Revs. Modern Phys. **29**, 683 (1957).

[25] Z. Fraenkel, Weizmann Institute of Science, Rehovoth, Israel, (private communication). The program used in this calculation is described in I. Dostrovsky, Z. Fraenkel, and G. Friedlander, Phys. Rev. **116**, 683 (1959), and I. Dostrovsky, P. Rabinowitz, and R. Blivins, *ibid.* **111**, 1659 (1958).

[26] Reference 23, p. 352.

by Blatt and Weisskopf[27] is

$$\mathcal{W}(E^*) = (\text{const})\exp[2(aE^*)^{\frac{1}{2}}]. \qquad (2)$$

The data have been replotted to show such a prediction as a straight line; Fig. 9 shows one such plot. The resulting values of $a$ at each angle and each energy are shown in Fig. 10. It appears that to within experimental error the values of $a$ are independent of the bombarding energy, but decrease with increasing angle of observation. This range of $a$, 2–5 Mev$^{-1}$, is not in qualitative disagreement with previous results from $N^{14}$ bombardment of other targets.[6]

Ericson[22] suggests that a more correct formula would be

$$\mathcal{W}(E^*) = (\text{const})(E^*)^{-2}\exp[2(aE^*)^{\frac{1}{2}}]. \qquad (3)$$

Representative data were fitted by substituting Eq. (3) in Eq. (1). It was found that the quality of the fits was not significantly changed, and that the principal result was to increase the values of $a$ by about 45%.

Another theoretical prediction for the energy spectra follows from the assumption of a constant "nuclear temperature" $T$ in the level density formula[28]

$$\mathcal{W}(E^*) = (\text{const})\exp(E^*/T). \qquad (4)$$

Figure 11 shows such fits as straight lines. Figure 12 shows that again there is no marked dependence upon bombarding energy.

We conclude that both of the above theoretical predictions fit the observed energy spectra about equally well, and that the shape of the spectrum observed at a given laboratory angle displays no marked dependence upon bombarding energy.
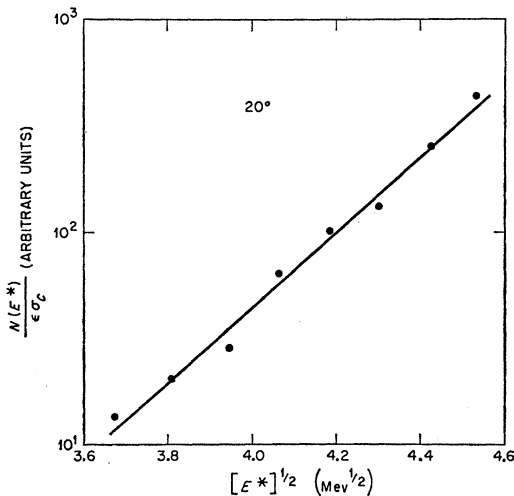


FIG. 9. An example of a proton energy spectrum, such as that of Fig. 6, plotted in such a manner that fits to the level density distribution $\exp[2(aE^*)^{\frac{1}{2}}]$ appear as straight lines. This case is 20° at a bombarding energy of 21.4 Mev.

[27] Reference 23, p. 371.
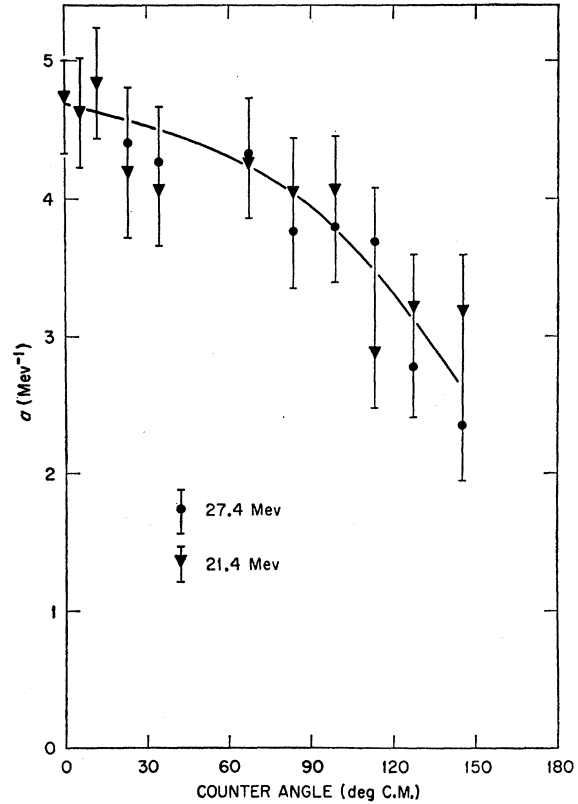[28] T. Ericson, Nuclear Phys. 11, 481 (1959).

FIG. 10. Plot of the level density parameter $a$ as a function of c.m. angle for protons from $F^{19}$ bombardment of 21.4- and 27.4-Mev $N^{14}$ ions.

## VI. FITS TO ANGULAR DISTRIBUTIONS

The theory of angular momentum effects in compound nucleus processes depends upon the fact that nuclei have finite moments of inertia and therefore finite intrinsic spins. To start with, $\mathbf{I} = \mathbf{l} + \mathbf{j}$, where $\mathbf{I}$ is the total angular momentum of the compound system, $\mathbf{l}$ is the orbital angular momentum of the final system, and $\mathbf{j}$ is the spin of the residual nucleus. If the average values of $I$ and $l$ are not small compared with the characteristic value of $j$ (say, $\sigma$) then there will be a tendency for $\mathbf{l}$ to line up parallel to $\mathbf{I}$, producing a peaking at 0° and at 180° in the c.m. system. The assumed distribution for $j$ is the Gaussian

$$pr(j) = (\text{const})(2j+1)\exp[-j(j+1)/(2\sigma^2)], \qquad (5)$$

for $j \lesssim \sigma^2$.[22] If the average values of $I$ and $l$ are not too large, one can use Knox's[8] approximate expansion of Eq. (13) of reference 10 for the energy and angular distribution:

$$W(\theta, E_p) \propto 1 + \tfrac{1}{3}\beta^2 P_2(\cos\theta) + (1/35)\beta^4 P_4(\cos\theta)$$
$$+ (5/4158)\beta^6 P_6(\cos\theta) + \cdots, \qquad (6)$$

where $\theta =$ counter angle in the c.m. frame of the initial collision, $\beta^2 = (2\sigma^2)^{-2}\langle I(I+1)\rangle_{\text{av}}\langle l(l+1)\rangle_{\text{av}}$, $E_p = [M_r/(M_r+M_p)]\epsilon =$ proton kinetic energy in the center-of-
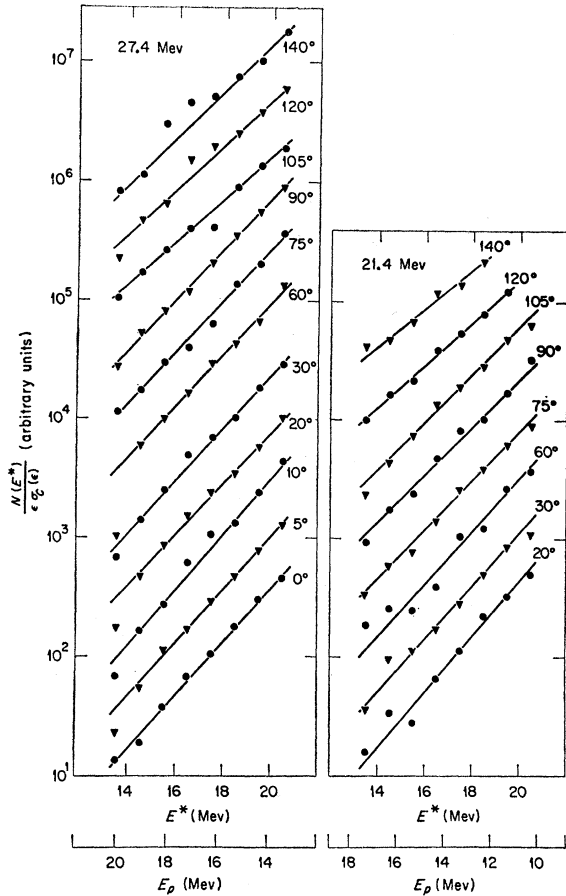
FIG. 11. The observed proton energy spectra plotted in such a way that fits to the level density distribution $\exp[E^*/T]$ appear as straight lines. The curves at different laboratory angles are arbitrarily displaced to avoid overlapping; each set of curves is labeled according to the laboratory bombarding energy.

mass frame of the initial collision, $M_r$= mass of residual nucleus, and $M_p$= proton mass.

Assumptions in Eq. (6) are the three conditions at the beginning of Sec. IV plus the following: (a) the validity of the classical approximation, including the neglect of the intrinsic spins of the observed proton and
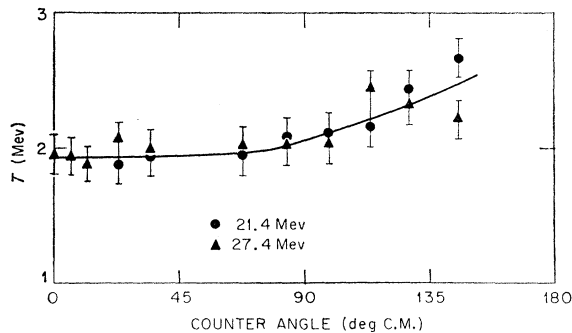


FIG. 12. Plot of the level density parameter $T$ as a function of c.m. angle for $N^{14}$ bombarding energies of 21.4 and 27.4 Mev.

the colliding nuclei, and (b) the condition that there is only weak coupling of the angular momenta of the compound and final systems. This last condition is expressed as[10]

$$\max[\langle I(I+1)\rangle_{av}, \langle l(l+1)\rangle_{av}] \lesssim (2\sigma^2)^2, \qquad (7)$$

and is well satisfied in the present cases.

To obtain a predicted energy and angular distribution containing as few arbitrary parameters as possible, the angular distribution of Eq. (6) was combined with the energy distribution of Eq. (4). Thus,

$$W'(\theta,E_p)$$
$$= (\text{const})(\epsilon)[\sigma_c(\epsilon)][\exp(E^*/T)]W(\theta,E_p). \qquad (8)$$

Here, the normalizing constant, the nuclear temperature $T$, and the cut-off spin $\sigma$ are the only arbitrary parameters and are all independent of $E_p$.

Figure 13 shows an approximate best fit to the 21.4-Mev results with Eq. (8). Here $\langle I(I+1)\rangle_{av}$ and
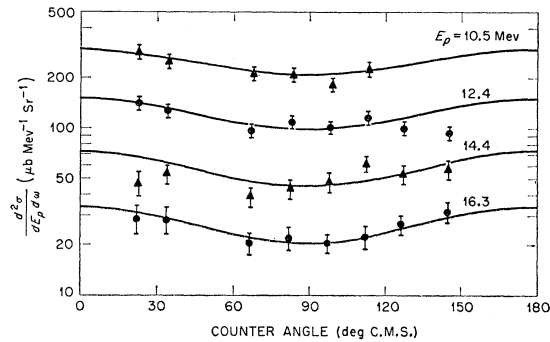


FIG. 13. Fit to the differential cross sections of Fig. 8 (21.4-Mev bombarding energy) by the modified Ericson-Strutinski formula of Eq. (8). The only adjustable parameters were $\sigma=3.18$, $T=2.14$ Mev. Note that the parameter $T$ fixes the normalization of the theoretical curves relative to each other.

$\langle l(l+1)\rangle_{av}$ were calculated as outlined and described in the Appendix. For this fit $T=2.14$ Mev and $\sigma=3.18$. This value of $T$ is consistent with the data at individual angles, as shown in Fig. 12. The consistency of this value of $\sigma$ with the moment of inertia $\mathcal{I}$ of the residual nucleus in Ericson and Strutinski's relation,[10]

$$\sigma^2 = \mathcal{I}T/\hbar^2, \qquad (9)$$

can be shown as follows: Use of Eq. (9) gives $\mathcal{I}$ for the $P^{32}$ nucleus at an excitation energy of about 25 Mev. For this nucleus $\mathcal{I}_{\text{rigid}}$ can be calculated on the basis of Hofstadter's charge distribution of the ground state of the similar nucleus $S^{32}$.[29] Then, within the error of the experimental fit, the above crude classical analysis yields

$$0.8 < \mathcal{I}/\mathcal{I}_{\text{rigid}} < 1.1. \qquad (10)$$

This is in accord with the prediction of Pik-Pichak[30]

[29] R. Hofstadter, Revs. Modern Phys. 28, 254 (1956).
[30] G. A. Pik-Pichak, Soviet Phys.—JETP 11, 557 (1960).

that even for rapidly rotating nuclei the moment of inertia approximates the rigid-body value.

For the comparison with the 27.4-Mev results appropriate values of $\langle I(I+1)\rangle_{\mathrm{av}}$ and $\langle l(l+1)\rangle_{\mathrm{av}}$ were calculated as above. The values of $\sigma$ and $T$ from the fit to the 21.4-Mev results were retained to provide some comparison with theoretical predictions, in spite of the lack of symmetry about 90°. The resulting theoretical prediction is shown in Fig. 14. It is seen that the fit is not nearly as good as that for the 21.4-Mev results, especially for the high-energy protons. This comparison is continued in the following section.

At both bombarding energies it is seen that the anisotropy of the proton angular distributions increases with increasing $E_p$, in accordance with the theoretical prediction. This is in contrast with the angular distributions of light particles from reactions induced in nickel by 160-Mev $O^{16}$ nuclei, where the opposite effect is observed.[8] A possible explanation for the latter effect lies in Ericson's prediction that for compound nuclei with high angular momentum the last light particle evaporated will carry off a disproportionately large amount of angular momentum.[22] If the last evaporated light particle has a relatively low average energy, this would cause an increase in the anisotropy constant as the light particle energy decreased, in accordance with observation. In the present case of reactions induced by 21.4-Mev and 27.4-Mev $N^{14}$ ions, perhaps the angular momenta, the multiplicity of emitted light particles, or the excitation energies are not sufficiently large for this effect to be important.

## VII. EFFECTS OF WEAKENED ASSUMPTIONS

As mentioned above, it is not required by energy considerations that all the observed protons correspond to transitions to the residual nucleus $P^{32}$. (Reactions which could contribute protons to the observed spectra are listed in Table II. It should be noted that factors inhibiting the emission of high-energy protons include the $Q$ value, the exponential increase of level density with excitation energy in the residual nucleus, the odd-even nature of the residual nucleus, and the reduced energy available after the first particle emission— especially if that particle must overcome a Coulomb barrier.) For the rest of this section it will be assumed that statistical reactions predominate, which implies that the particles are boiled off sequentially. Then the observed protons can be divided into those which are boiled off before any other particle ("primary" protons) and subsequent ("secondary") protons. The above theoretical predictions thus apply to primary protons. In the observed energy spectra it would be expected that, due to the lowered excitation of the compound system, the secondary protons will contribute proportionately more to the low-energy end than to the high-energy end. Thus, the values of $a$ and $T$ reported above would represent limits on the true values (averaged over
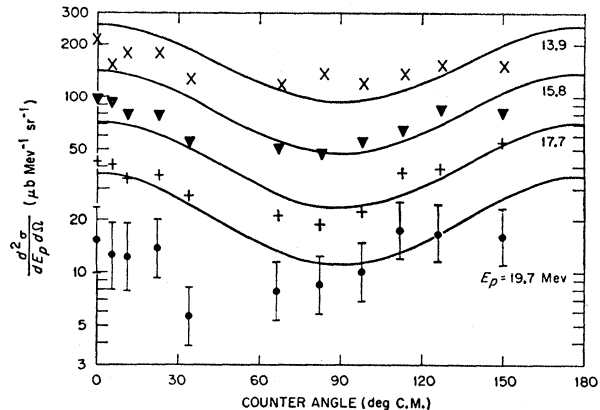


FIG. 14. Fit to the differential cross sections of Fig. 7 (27.4-Mev bombarding energy) for the same equation and adjustable parameters as the fit in Fig. 13, but with the angular momentum parameters appropriate to this case.

the residual nuclei involved): An upper limit on $a$ and a lower limit on $T$. In the angular distributions, it would be expected that a sharing of the excess angular momentum of the compound system among more than one emitted particle would decrease the anisotropy of the observed proton angular distributions. Given the observed anisotropy, since $\langle I(I+1)\rangle_{\mathrm{av}}$ and $\langle l(l+1)\rangle_{\mathrm{av}}$ would be unaffected, the value of $\sigma$ reported above would become an upper limit on the true value.

Next to be considered is possible weakening of the assumption that all protons are emitted by compound-nucleus process. In this light the change of $a$ and $T$ with counter angle suggest an admixture of a direct interaction process, with the protons coming from the target nucleus.[31] This would also be consistent with the excess of protons emitted into the backward hemisphere, especially at the 27.4-Mev bombarding energy. A direct-interaction admixture would also predict the observed increase in the backward peaking with increased proton energy and with increased bombarding energy. It is not obvious, however, how the independence of spectrum shape from bombarding energy fits into this picture.

TABLE II. Proton-producing reactions from $N^{14}$ bombardment of $F^{19}$ which have $Q>0$. Column (2) gives the respective $Q$ values. The difference between the $Q$ values of each reaction and the $(N^{14},p)$ reaction are listed in column (3).

| (1)<br>Reaction | (2)<br>$Q$<br>(Mev) | (3)<br>18.45 Mev$-Q$<br>(Mev) |
|---|---|---|
| $F^{19}(N^{14},p)P^{32}$ | 18.45 | 0 |
| $F^{19}(N^{14},pn)Si^{31}$ | 10.45 | 8.0 |
| $F^{19}(N^{14},2p)P^{31}$ | 9.82 | 8.6 |
| $F^{19}(N^{14},p\alpha)Al^{28}$ | 8.56 | 9.9 |
| $F^{19}(N^{14},pd)Si^{30}$ | 5.46 | 13.0 |
| $F^{19}(N^{14},n2p)Si^{30}$ | 3.16 | 15.3 |
| $F^{19}(N^{14},pt)Si^{29}$ | 1.09 | 17.4 |

[31] L. Madansky and G. E. Owen, Phys. Rev. **99**, 1608 (1955).

In view of (a) the reasonable fit of the 21.4-Mev results to the predictions of the angular momentum effects in compound nucleus processes, (b) the multiplicity of reactions contributing the observed protons, and (c) the above suggestion of an admixture of direct interaction processes, it would appear that further work would be required to elicit the precise nature of the mechanism producing protons from $N^{14}$ bombardment of $F^{14}$ at these energies.

## ACKNOWLEDGMENTS

The author gratefully acknowledges the suggestions and continual encouragement of A. Zucker. The advice of C. D. Goodman and J. B. Ball regarding the proportional counter design, the electronics, and the data-processing codes is greatly appreciated. It is a pleasure to acknowledge valuable discussions with D. Bodansky, T. Ericson, and I. Halpern. Thanks are extended to T. L. Emmer for advice on the electronics, A. W. Riikola and H. L. Dickerson for steady operation of the cyclotron, G. A. Palmer for assistance in taking the data, and J. G. Harris for construction of the apparatus.

## APPENDIX

In Sec. VI it was mentioned that theoretical predictions of the mean-square orbital angular momentum $\langle l(l+1)\rangle_{av}$ were calculated by means of the optical model, while $\langle I(I+1)\rangle_{av}$ was calculated by interpolation from Thomas' barrier penetration calculations.[32] It was felt that taking the wave mechanical nature of the collisions into account would yield more accurate results than the sharp-barrier cutoff formulas used by Ericson and Strutinski,[10] of the form

$$\langle I^2 \rangle_{av} = \mu \hbar^{-2}(E_{c.m.} - B)R^2. \qquad (A.1)$$

Here $E_{c.m.}$ is the channel energy of the collision or evaporation, $\mu$ is the reduced mass, $B$ the Coulomb barrier, and $R$ the interaction radius. A brief description of the methods used in the present work follows.

### Optical Model Method

The code used was that written for an IBM 704 by Bassel and Drisko[33]; it is similar to the code of Melkanoff et al.[34] This code calculated wave amplitudes from which it was easy to obtain the partial wave transmission coefficients $T_l$. Then $\langle l(l+1)\rangle_{av}$ was calculated as

$$\langle l(l+1)\rangle_{av} = \frac{\sum (l)(l+1)(2l+1)T_l}{\sum (2l+1)T_l}. \qquad (A.2)$$

The parameters used in the optical model calculations were those suggested by Bassel[35] as giving reasonable

[32] T. D. Thomas, Phys. Rev. 116, 703 (1959).
[33] R. H. Bassel and R. M. Drisko, reference 3, p. 212.
[34] M. A. Melkanoff, J. S. Nodvik, D. S. Saxon, and R. D. Woods, Phys. Rev. 106, 793 (1957).
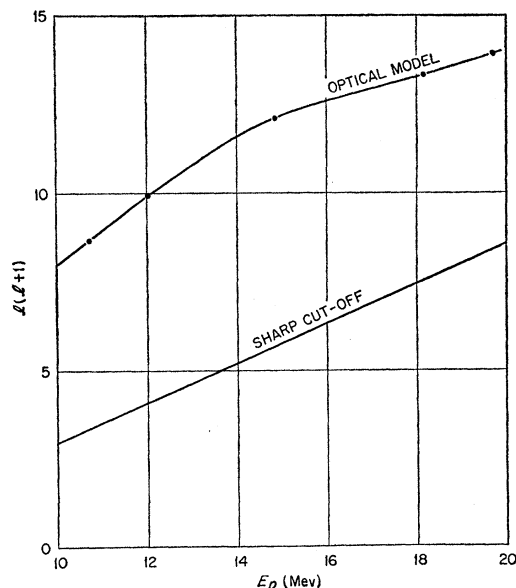[35] R. H. Bassel, Oak Ridge National Laboratory (private communication).

FIG. 15. Plot of the mean-square orbital angular momentum $\langle l(l+1)\rangle_{av}$ for the inverse reaction, proton bombardment of $P^{32}$, as a function of the c.m. kinetic energy of the proton. The curve labeled "optical model" was calculated as described in the Appendix; the dots represent the individual calculated points. The curve labeled "sharp-cutoff model" was calculated from Eq. (A.1) with $R = 1.5\ A^{\frac{1}{3}}$ fermi.

fits for elastic proton scattering in the mass region of interest. In the notation of reference 34, these parameters were:

$$V = 57.9\ \text{Mev} - 0.62\ E_L,$$
$$W = 6.0\ \text{Mev} + 0.155\ E_L,$$
$$R = 1.3\ A^{\frac{1}{3}}\ \text{f},$$
$$a = 0.42\ \text{f},$$

where $E_L$ is the proton energy in the laboratory system. While the parameters of optical model fits in general are nonunique, in the proton energy range of interest here the optical model is capable of giving simultaneous qualitative fits to the total reaction cross section and polarization, as well as to the differential cross section of elastic scattering.[36]

The results for the $\langle l(l+1)\rangle_{av}$ of protons boiled off with a residual nucleus of $P^{32}$ are shown in Fig. 15 and were used in the calculations of the theoretical curves of Figs. 13 and 14. Shown for comparison purposes are the predictions of Eq. (A.1) with $R = 1.5\ A^{\frac{1}{3}}$ f and $B = zZe^2/R$. For smaller values of $R$ the difference between the two curves would be even more marked.

### Barrier Penetration Method

Unfortunately, the present form of the Bassel-Drisko code is not yet suitable for values of $\eta = Z_1 Z_2 e^2 / \hbar v$ greater than about six, so that values of $\langle I(I+1)\rangle_{av}$

[36] V. Meyer and N. M. Hintz, Phys. Rev. Letters 5, 207 (1960).

for the $N^{14}$—$F^{19}$ collision could not be estimated by optical model calculations, such as were used to analyze $N^{14}$—C and $N^{14}$—$Be^9$ elastic scattering.[33] Still available were the heavy-ion barrier-penetration calculations of Thomas,[32] which used a square-well potential with radius $1.5\ A^{\frac{1}{3}}$ f. Interpolation from Thomas' results was accomplished as follows:

(1) For each of the collisions $C^{12}$—$Al^{27}$, $O^{16}$—$Al^{27}$, $N^{14}$—$Al^{27}$ in Thomas' Table I, values of $\bar{I}$ were interpolated for the same values of $\epsilon/B$ as for the $N^{14}$—$F^{19}$ collision.

(2) By extrapolation on the basis of the parameter

$\eta$ values of $\bar{I}$ were determined for the two energies of the $N^{14}$—$F^{19}$ collision.

(3) $\bar{I}$ and $\langle I(I+1)\rangle_{\text{av}}$ were related by means of Thomas' Fig. 5, which shows partial wave absorption cross sections for $Al^{27}$—$C^{12}$ collisions at four energies. From this figure $\langle I(I+1)\rangle_{\text{av}}/(\bar{I})^2$ was calculated as a function of $\eta$; interpolation for the $N^{14}$—$F^{19}$ case gave the results shown in Table I.

These stages of interpolation are summarized in the following equation:

$$[I(I+1)]_{\text{N-F},\epsilon/B,\eta} = [\bar{I}]^2_{\text{X-Al},\epsilon/B,\eta}[I(I+1)/(\bar{I})^2]_{\text{C-Al},\eta}. \tag{A.3}$$

# Beta-Gamma Directional Correlation in $Eu^{154}$†

K. S. R. Sastry, R. F. Petry, and R. G. Wilkinson

*Indiana University, Bloomington, Indiana*

(Received March 9, 1961)

The energy dependence of the beta-gamma angular correlation between the outer beta-ray group of $Eu^{154}$, $W_0=1.86$ Mev, and the 123-kev gamma ray of the daughter $Gd^{154}$ has been measured with a shaped magnetic field beta-gamma coincidence spectrometer. A negative correlation coefficient, accurate to about 5%, is obtained which ranges from $-0.10$ to $-0.17$ in the energy region 0.80 to 1.60 Mev. It is shown that the modified $B_{ij}$ approximation must be relaxed to explain the data. The nuclear parameters (Kotani's notation) which result are: $x=-0.24\pm0.05$, $u=+0.05\pm0.03$, $Y=+0.76\pm0.08$. These values are compared with those which have been reported for $Eu^{152}$: $x=u=0$, $Y=0.69\pm0.06$.

## INTRODUCTION

OF particular interest in beta-gamma angular correlation studies are certain $3^-(\beta)2^+$ decays from odd-odd to even-even nuclei which are characterized by abnormally long comparative half-lives. Kotani[1] has suggested that this situation may arise from cancellation among the nuclear matrix elements or from additional selection rules, such as those associated with $K$ forbiddenness. Deviations from the $\xi$ approximation are expected in these cases, which should be manifest in experiments as an energy-dependent shape factor and a large beta-gamma correlation coefficient $\epsilon$. The highest energy beta groups of $Eu^{152}$ and $Eu^{154}$ appear to be examples of this effect, since both have large comparative half-lives ($\log ft\simeq12$) and both are nonunique first-forbidden decays with nonstatistical beta-ray shapes.[2] Beta-gamma angular correlation studies in $Eu^{152}$ support this view. It has been shown,[3] for example, that the energy dependence of the large negative correlation coefficient is adequately described by the modified $B_{ij}$ approximation

$(x=u=0,\ Y\neq0)$, and that the matrix element ratio,[4] $Y=0.69\pm0.06$, is in good agreement with the value obtained in the same approximation from the spectrum shape determination of Langer and Smith.[2] In this case it seems well established that $u$ and $x$ are suppressed relative to $B_{ij}$ by some selection rule effect. The slowness of the transition is probably associated with the fact that $_{64}Gd^{152}$, although spherical, is close to the transition region (neutron numbers 88–90) between spherical and deformed even-even nuclei.[5]

For a more detailed understanding of the selection rule effect it seems desirable to have available the beta-gamma correlation data in the companion case of $Eu^{154}$. In this decay, the highest energy beta group is a once-forbidden transition from a $3^-$ initial state in $Eu^{154}$ to a $2^+$ final state in $Gd^{154}$, and is followed by a 123-kev $E2$ gamma-transition to the $Gd^{154}$ ground state.[6] The large comparative half-life, $\log ft=12.4$, is probably associated with the change in the deformation parameter

† Supported by the Joint Program of the Office of Naval Research and the U. S. Atomic Energy Commission.

[1] T. Kotani, Phys. Rev. 114, 795 (1959).

[2] L. M. Langer and D. R. Smith, Phys. Rev. 119, 1308 (1960).

[3] H. J. Fischbeck and R. G. Wilkinson, Phys. Rev. 120, 1762 (1960).

[4] The notation of reference 1 will be used throughout this paper. A discussion of the modified $B_{ij}$ approximation as it applies to these measurements is given in reference 3.

[5] R. K. Sheline, Rev. Modern Phys. 32, 1 (1960).

[6] *Nuclear Data Sheets*, National Academy of Sciences, National Research Council (U. S. Government Printing Office, Washington, D. C.).